Direct measurement of dispersive nonlinearities in GaAs

Y. H. Lee, A. Chavez-Pirson, B. K. Rhee, H. M. Gibbs, A. C. Gossard, and W. Wiegmann

Citation: Applied Physics Letters **49**, 1505 (1986); doi: 10.1063/1.97315
View online: http://dx.doi.org/10.1063/1.97315
View Table of Contents: http://scitation.aip.org/content/aip/journal/apl/49/22?ver=pdfcov
Published by the AIP Publishing

Direct measurement of dispersive nonlinearities in GaAs

Y. H. Lee, A. Chavez-Pirson, B. K. Rhee, and H. M. Gibbs
Optical Sciences Center, University of Arizona, Tucson, Arizona 85721

A. C. Gossard and W. Wiegmann
AT&T Bell Laboratories, Murray Hill, New Jersey 07974

(Received 22 August 1986; accepted for publication 6 October 1986)

Nonlinear refractive index changes in 299 Å multiple quantum well GaAs were obtained directly by measuring Fabry–Perot transmission peak shifts. These changes crosscheck those obtained by Kramers–Kronig transformations of the nonlinear absorption under identical pumping conditions. High intensities saturate the exciton, so that nonlinear refractive index changes are dominated by nonresonant contributions. Thermal refractive index changes were also measured directly.

Dispersive nonlinearities are known to be responsible for optical bistability[1] and optical logic gate action in many semiconductors such as GaAs,[2] InSb,[3] and CdS.[4] Several attempts have been made to measure the dispersive nonlinearities in semiconductors. Recently, Downer *et al.* measured interference fringe shifts to obtain refractive index changes in Si on sapphire.[5] Olbright *et al.* employed a Twymann–Green interferometric technique to obtain refractive index changes in color filters.[6] Miller *et al.* measured nonlinear refractive index changes by measuring the Gaussian beam distortion due to self-defocusing in InSb.[7] Baumert *et al.* used very thin crystal prisms of CdS and measured beam deflection due to a nonlinear refractive index change.[8] A more common technique is to measure band-edge absorption changes as a function of pump intensities and then perform Kramers–Kronig transformations to obtain the corresponding refractive index changes. But a Kramers–Kronig transformation needs the absorption changes at all frequencies. This limits the accuracy and validity of such a transformation, if absorption changes are measured in a too-narrow region. For GaAs, Chemla *et al.* examined multiple quantum well GaAs nonlinear absorption at low intensities and calculated the nonlinear refractive index change using a Kramers–Kronig relation.[9]

In this letter, we report direct measurement of nonlinear refractive index changes by monitoring nonlinear Fabry–Perot (FP) transmission peak shifts due to dispersive nonlinearities in GaAs at room temperature. In addition, nonlinear absorption changes in the vicinity of the band edge were measured under identical pumping conditions, and the corresponding nonlinear refractive index changes were calculated by Kramers–Kronig transformations. These two data sets obtained by different methods agree well, demonstrating the validity of the Kramers–Kronig technique under quasi-steady-state pumping conditions. At low pump intensities, the small index changes arising from exciton saturation were evident but fall off rapidly as one moves away from the exciton wavelength. At higher pump intensities, the index changes have relatively broad spectra extending to longer wavelengths (>900 nm), suggesting contributions from band filling and the screening of Coulomb enhancement of continuum states.

The GaAs multiple quantum well (MQW) sample was grown by molecular beam epitaxy and consisted of 61 periods of 299 Å GaAs and 99 Å AlGaAs layers supported by two windows of 2930-Å-thick and 2015-Å-thick AlGaAs. The sample was then sandwiched between two dielectric mirrors (90% reflectivity) on sapphire substrates to form a FP étalon. The free-spectral range (FSR) of the FP étalon was about 230 Å. The FP étalon was reasonably flat over the sample, and FP transmission peaks of the étalon were located at 876 ± 4 nm and 890 ± 6 nm. These slight variations in transmission peak positions are attributed to the nonflatness of the sapphire substrates and the minute wedge introduced during the selective etching of the sample. The exciton peak of this 299-Å MQW GaAs sample is at 8696 Å. Since its quantum well thickness is slightly larger than the exciton diameter, its characteristics should be similar to those of bulk GaAs.

Initially, the fluorescence (broadband source) from LDS 821 dye jet was aligned to monitor the spot pumped by the dye laser and was fed into an optical multichannel analyzer (OMA). During the experiment it was found that the photoluminescence from the 15-μm-diam focused pump spot on the GaAs étalon was strong enough to be detected at the OMA. It was verified that the FP transmission peak seen using the photoluminescence was at the same wavelength as the one seen using the dye fluorescence. Consequently, one can use the photoluminescence from the sample itself as a broadband probe source, if one is only interested in the FP peak wavelength. Since the photoluminescence is due to the carriers generated by the pump beam, the pump and probe are automatically aligned.

When an Ar laser was used as a pump source, thermal effects were observed as a function of pulse length and identified by their red shift (positive refractive index change) of the FP transmission peak. To minimize the thermal effects, the rest of the experiment was performed using a dye laser pump at 821 nm. Up to the maximum pump intensity, unwanted red shifts due to the infrared pump were checked and avoided by reducing the duty cycle of the pump beam (10 kHz). The pulse width of the pump beam was 1 μs. The maximum pump power was 90 mW before the étalon, and 20% of the power was assumed to be absorbed by the sample to excite the carriers responsible for the nonlinear refractive index change.

Figure 1 shows typical nonlinear FP transmission curves seen by the photoluminescence at high and low pump

 0003-6951/86/481505-03$01.00

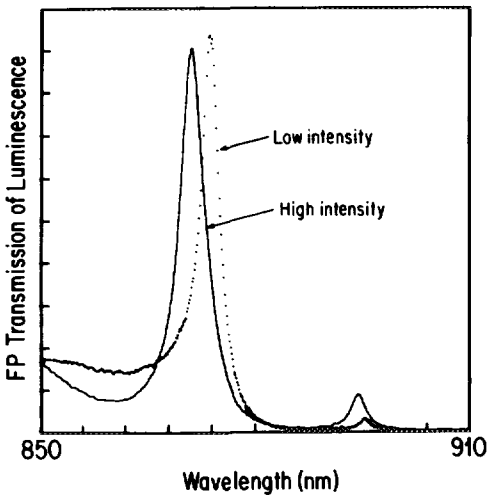

FIG. 1. Typical FP transmission peaks seen by the photoluminescence of GaAs at low and high pump intensities after normalization.

intensities. With two FP peaks at one étalon point, one can measure the free-spectral range which corresponds to a 2π phase change. Carriers generated by absorption of laser light introduce negative nonlinear refractive index changes. The FP transmission peak then blue shifts in the case of a defocusing nonlinearity such as that of GaAs. If there is an increase in the GaAs lattice temperature, the positive thermal refractive index change red shifts the peaks. By measuring this shift one can calculate Δn; if there is no dispersion

$$\Delta\phi = 2\pi\Delta\lambda\,/\mathrm{FSR}(\lambda); \quad \Delta n = \lambda\Delta\phi/4\pi L, \tag{1}$$

where $\Delta\lambda$ is the FP transmission peak shift in wavelength. If there is dispersion, one must know the phase variation in the nonlinear FP étalon as a function of wavelength. This can be obtained by measuring the FSR for many different wavelengths. In this case one can calculate the phase variation by knowing the linear refractive index $n(\lambda)$ of GaAs[10] and the étalon thickness. Figure 2 is the calculated phase function $\phi(\lambda)$ of the étalon assuming 2.9-μm GaAs and 1.35-μm air gap. It reproduces the measured FSR variation successfully. With this curve, one can deduce $\Delta\phi$ by calculating the phase difference between the shifted FP peak position and the reference one. If a FP peak initially at λ_0 is shifted to λ_{NL} after

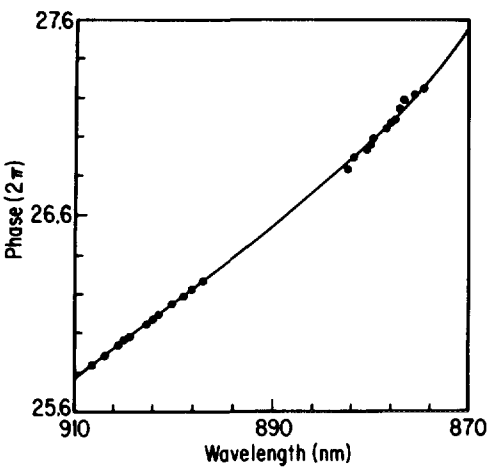

FIG. 2. Phase function of a GaAs étalon. Dots are plotted using measured FSR data.

absorption of laser light, one can say that the phase of the FP étalon at λ_0 at low pump intensity is equal to that at λ_{NL} at high pump intensity. Then the nonlinear phase change at λ_{NL} can be obtained simply as the difference of the phases at two wavelengths $[\phi(\lambda_0) - \phi(\lambda_{NL})]$, and Δn follows from Eq. (1). For wavelengths longer than 874 nm, the measurement error of the nonlinear refractive index was 0.002. Since the phase function was tested self-consistently in this region, the accuracy was limited by the resolution of the OMA, 1.5 Å. For wavelengths shorter than 873 nm, the error was about 0.006. An extrapolated phase function was used in this region. If the linear refractive index were known more precisely in the band-gap region, the measurement accuracy could be improved.

The nonlinear absorption changes in Fig. 3(a) were obtained by a quasi-cw pump-and-probe experiment. The wavy structures in curves 5 and 6 are from the incomplete antireflection coating of the sample. The wavelength of the pump laser was the same (821 nm) as that used in the direct index measurement. At pump powers less than 1.1 mW, the nonlinear changes result almost entirely from the exciton peaks. At higher pump powers (>2 mW), the exciton absorption is completely saturated due to plasma screening, because there is more than one electron-hole pair per unit exciton volume (1 mW on 15 μm diameter corresponds to Mott density, $\simeq 1\times10^{17}$ electron-hole pairs per cm^3). The nonlinear refractive index change, however, does not saturate, rather it continues to increase with the pump intensity. In Fig. 3(a), one can see characteristically different behavior of absorption changes for the curves b through e compared to that of curve a. The changes at higher pump powers may be largely attributed to nonresonant contributions from band filling

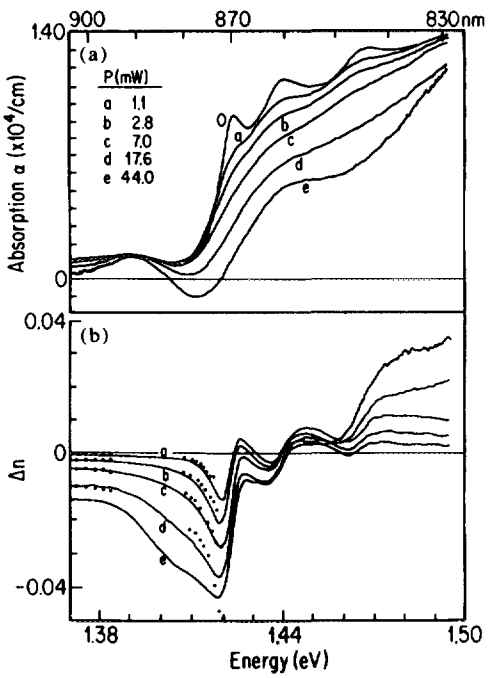

FIG. 3. (a) Nonlinear absorption spectra measured by quasi-cw pump-and-probe experiment. (b) Nonlinear refractive index changes (Δn) obtained directly from the FP peak shifts (dots). Solid curves are obtained by Kramers–Kronig transformations of measured $\Delta\alpha$. For example, curve a in (b) is calculated from $\Delta\alpha$ between reference absorption spectrum, curve 0 in (a), and nonlinear absorption spectrum, curve a in (a).

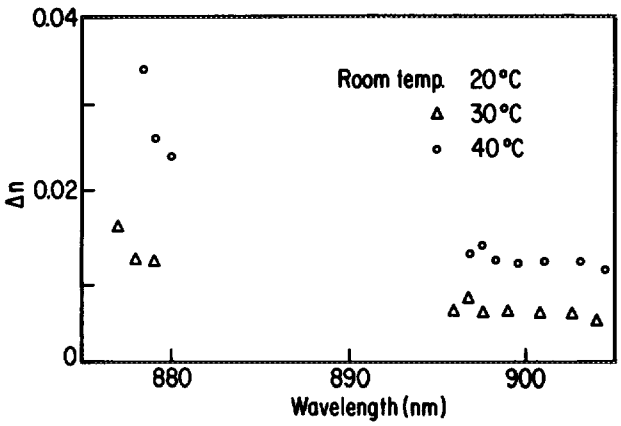

FIG. 4. Thermal contribution to refractive indices in the vicinity of the band edge of 299 Å MQW GaAs.

and the screening of Coulomb enhancement of continuum states as in bulk GaAs.[11,12]

Optical bistability was observed using 10 mW for the region of large nonlinear refractive index change (872–878 nm). This input power exceeds the intracavity power (<3 mW) needed to saturate the excitons, suggesting that nonresonant nonlinearities are as important as the excitonic nonlinearity for optical bistability. One needs $\Delta n > 0.01$ for dispersive optical bistability for the current étalon design, consistent with the observation of optical bistability with 10 mW. With 40 mW, optical bistability was observed over a wide spectral region (866–883 nm), even inside the exciton peak. The optical bistability in this power regime would be interpreted as mixed dispersive and absorptive bistability.

Thermal refractive index changes at the band edge of 299 Å MQW GaAs were measured similarly by looking at FP transmission peak shifts as a function of lattice temperature. As shown in Fig. 4, positive refractive index changes[13] occur below the band gap as a result of band-gap shrinkage with increase of lattice temperature. A 20° increase in lattice temperature introduces a positive contribution in the vicinity of the band edge large enough to compensate the high-intensity negative one. For nonlinear optical devices based on dispersive nonlinearities in GaAs, the operating temperature should be stabilized to about 1° for reliable operation.

In summary, the dispersive nonlinearities in GaAs were measured directly by observing the FP transmission peak shift using photoluminescence as a broadband probe source. At room temperature, the nonresonant contributions are as important as the excitonic effects in explaining nonlinear index changes of 299 Å MQW GaAs. Thermal contributions to the refractive index change were measured directly to give thermal stability conditions on nonlinear étalon devices based on GaAs.

The Arizona portion of this research was supported by the National Science Foundation, the Air Force Office of Scientific Research, the Army Research Office, and the Optical Circuitry Cooperative.

[1] H. M. Gibbs, *Optical Bistability: Controlling Light with Light* (Academic, New York, 1985).
[2] H. M. Gibbs, T. Venkatesan, S. L. McCall, A. Passner, A. C. Gossard, and W. Wiegmann, Appl. Phys. Lett. **34**, 511 (1979); J. L. Jewell, Y. H. Lee, M. Warren, H. M. Gibbs, N. Peyghambarian, A. C. Gossard, and W. Wiegmann, Appl. Phys. Lett. **46**, 918 (1985).
[3] D. A. B. Miller, S. D. Smith, and A. Johnston, Appl. Phys. Lett. **35**, 742 (1979).
[4] M. Dagenais, J. Opt. Soc. Am. **72**, 1835 (1982); M. Dagenais, Appl. Phys. Lett. **43**, 742 (1983).
[5] M. C. Downer and C. V. Shank, Phys. Rev. Lett. **56**, 761 (1986).
[6] G. Olbright and N. Peyghambarian, Appl. Phys. Lett. **48**, 1184 (1986).
[7] D. A. B. Miller, C. T. Seaton, M. E. Price, and D. S. Smith, Phys. Rev. Lett. **47**, 197 (1981).
[8] R. Baumert, I. Broser, and K. Buschick (unpublished); for thin-prismatic measurement technique, see I. Broser, R. Broser, E. Beckman, and E. Birkish, Solid State Commun. **39**, 1209 (1981).
[9] D. S. Chemla, D. A. B. Miller, P. W. Smith, A. C. Smith, A. C. Gossard, and W. Wiegmann, IEEE J. Quantum Electron. **QE-20**, 265 (1984).
[10] A. N. Pikhtin and A. D. Yas'kov, Sov. Phys. Semicond. **12**, 622 (1978).
[11] Y. H. Lee, A. Chavez-Pirson, S. W. Koch, H. M. Gibbs, S. H. Park, J. Morhange, N. Peyghambarian, L. Banyai, A. C. Gossard, and W. Wiegmann (unpublished).
[12] L. Banyai and S. W. Koch, Z. Physik, **B63**, 283 (1986).
[13] J. L. Jewell, H. M. Gibbs, and S. S. Tarng, Appl. Phys. Lett. **40**, 291 (1982).